THE LATEST TEST OF THE SPACE-WISE APPROACH FOR GOCE DATA ANALYSIS

F. Migliaccio[(1)], M. Reguzzoni[(2)], F. Sansò[(3)], N. Tselfes[(3)], C. C. Tscherning[(4)], M. Veicherts[(4)]

[(1)] DIIAR - Politecnico di Milano - Piazza Leonardo da Vinci, 32 - 20133 Milano - Italy
[(2)] Geophysics of the Lithosphere Dept. - Italian National Institute of Oceanography and Applied Geophysics (OGS) c/o Politecnico di Milano, Polo Regionale di Como - Via Valleggio, 11 - 22100 Como - Italy
[(3)] DIIAR - Politecnico di Milano, Polo Regionale di Como - Via Valleggio, 11 - 22100 Como - Italy
[(4)] University of Copenhagen, Juliane Maries Vej 30 , 2100 Copenhagen - Denmark

ABSTRACT

A new set of E2E (end-to-end) simulated data for the GOCE mission has been recently produced by the European Space Agency and used for extensive testing of the procedures for the estimation of the gravity field. These data set spans 60 days and includes the satellite state vector data and orientation parameters, the measured gravity gradients and the measured non gravitational accelerations. These data have been contaminated by realistic in-flight calibration noise and other systematic effects, like biases, which make the analysis more difficult and meaningful.

The space-wise solution procedure has been applied to the E2E data with very promising results. However some routines of the procedure had to undergo further tuning with respect to previous experiments. In fact, calibration methods have been used to estimate biases in the common-mode accelerations and long wavelength effects in the gravity gradients, before these data could enter the basic processing chain. In this experiment for the first time a real combination of the energy integration solution and the gradiometry solution has been achieved, which permits also the accurate estimation of low degree coefficients. Moreover it has been found that the information of the GOCE data, according to this simulation scenario, can be used to resolve for coefficients beyond degree 200 with a commission geoid error of the order of centimetres. This result is not an assessment of the performance of the GOCE mission, however it is a positive test of the effectiveness of the space-wise approach for processing the GOCE data.

1. THE GOCE MISSION

GOCE (Gravity field and steady-state Ocean Circulation Explorer) is a satellite gradiometry mission designed by ESA (European Space Agency), which is scheduled to be launched in 2007 (ESA, 1999). The main goal of the mission is the determination of a spherical harmonic model of the earth gravitational field with high accuracy and spatial resolution. The main instrument on board the satellite will be a tri-axial gradiometer that is composed by three pairs of electrostatic accelerometers assembled according to orthogonal axes. This configuration allows for the measurement of the second derivatives of the potential along the satellite orbit (the so-called gravitational gradients). More information on the gravity field will be derived from the tracking of the satellite orbit by means of the on board GPS receiver. The orbit tracking data will be combined with the measurements of the non-gravitational forces acting on the satellite, obtained by the gradiometer common mode accelerations. The different sources of information are complementary to each other: the gravitational gradients mainly provide information on the medium and high degrees of the spherical harmonic expansion (i.e. the high frequency details of the field), while the satellite orbit tracking allows to estimate the lowest degrees (i.e. the behaviour of the field at low frequencies) with better accuracy.

Three different approaches have been developed for the estimation of a gravity field model from the GOCE mission: the direct approach (Abrikosov and Schwintzer, 2004), the time-wise approach (Pail et al., 2005) and the space-wise approach (Migliaccio et al., 2004a) that is realized by the Politecnico di Milano in cooperation with the University of Copenhagen. These specialized data analysis methods are part of the work made by EGG-C (European GOCE Gravity Consortium) (Rummel et al., 2004). In this paper the state of the space-wise approach is presented and its performance is evaluated by a full simulation solution, showing that it is capable of processing the satellite data.

2. THE SPACE-WISE APPROACH

The idea of the space-wise approach is to exploit the spatial correlation of the gravitational field by creating a grid of gravity related observables on a spherical mesh. This is obtained by the least squares collocation method. Afterwards the coefficients of a spherical harmonic expansion are estimated by applying algorithms of harmonic analysis.

Before the procedures of gridding and harmonic analysis are run a pre-processing of the data is required. This is due to the particular characteristics of the GOCE

Proc. 'The 3rd International GOCE User Workshop', ESA-ESRIN, Frascati, Italy,
6–8 November 2006 (ESA SP-627, January 2007)

data and of the space-wise approach. This pre-processing regards both the satellite orbit tracking data and the gradiometer data and, in order to correct for initial approximations, iterations are also made.

2.1 Potential estimate along the orbit

The first pre-processing step regards the orbit tracking data, i.e. the positions and velocities recovered from the tracking of the GOCE orbit by GPS satellites, together with the measurements of the non-gravitational accelerations. With this data the potential is directly estimated along the orbit at a point $\underline{x}_e = \begin{bmatrix} x_e & y_e & z_e \end{bmatrix}^T$, via the energy conservation method (Jekeli, 1999; Visser et. al., 2003):

$$E_0 + T(\underline{x}_e) = \frac{1}{2}\underline{v}_e^T \underline{v}_e - \frac{1}{2}\omega_e^2\left(x_e^2 + y_e^2\right) + \int_0^t \underline{f}_e \cdot \underline{v}_e \, dt \,, \quad (1)$$

where E_0 is an unknown integration constant, $\underline{v}_e = \begin{bmatrix} v_{x_e} & v_{y_e} & v_{z_e} \end{bmatrix}^T$ is the velocity vector in the ERF (Earth-fixed Reference Frame), ω_e is the earth rotation rate. The subscript e denotes ERF, the symbol T denotes transposed. The integral represents the friction, i.e. the energy loss due to non gravitational accelerations, where $\underline{f}_e$ is the vector of non gravitational forces. In practice this integral is numerically evaluated on the basis of the constant sampling rate of the data.

2.2 Low degree reference model

A low degree reference model is needed, in order to be used for the Wiener filter (see paragraph 2.3). Therefore a "small space-wise approach" is applied to only the along track potential estimates. An a-priori reference model is subtracted from this data and then a spherical grid of predicted values of the gravitational potential, at mean satellite altitude, is computed. This is achieved by performing least squares collocation on local patches of data (Tscherning, 2005). Then by applying numerical integration on this grid, corrections to the original reference model are computed for the low harmonic degrees and a new model is generated.

The information on the lowest harmonic degrees of the gravity field from the potential is much better than the one obtained from the gradients. Therefore the coefficients of the lowest degrees of this estimated model are included in the final model, meaning that no further corrections are estimated for these coefficients when the gradients enter the processing.

2.3 Wiener filter

The gradients observations noise is high and has a very long correlation length in time. This is very inconvenient for the gridding procedure, where data series (satellite orbit arcs) of limited length in time are considered, inside localized patches. This "local gridding" is made because a global gridding with all the data is numerically impossible. Therefore a time-wise filter is performed (Albertella et al., 2004), which results in a significant reduction of this noise. Besides, error estimates of the filtered data are computed, which can be used in the subsequent gridding procedure. This result is important because accurate information on the covariance functions of the observations noise is not available.

The low degree reference model, estimated at the previous step, is subtracted both from the gradients observations and from the potential estimates. In this way the data are rendered zero mean and stationary. A model that describes the peaks of the residual gravity field is also subtracted, for the purpose of statistical homogenisation (Migliaccio et al., 2004c). This model is computed by creating a grid of second radial derivatives of the gravitational potential from an a-priori model, then by selecting the peaks of this field and finally by applying harmonic analysis to these peaks.

It has to be remarked that the Gradiometer Reference Frame (GRF) (x,y,z being the instrumental axes) does not coincide with the Local Orbital Reference Frame (LORF) (ξ: almost along-track; η: cross-track; r: radial). Therefore the observed gravitational gradients cannot be considered a signal stationary in time and the Wiener filter should be applied to the corresponding quantities in the LORF system (Albertella et al., 2004). A direct rotation cannot be applied to the gravitational tensor because the large error in the non-diagonal components of the tensor would be propagated to all the other components. For this reason, a preliminary estimate of the diagonal components is performed in LORF, to be used in the Wiener filter, by ignoring the effects on the rotation due to the non-diagonal terms. In fact this can be made by applying the proper rotation operator, but setting to zero the gradients whose contribution is not desired. These terms will be iteratively corrected (Migliaccio et al., 2004b).

These data are then transformed into the frequency domain and filtered by a Wiener filter (Papoulis, 1984) along the orbit. For a certain frequency f, one can write:

$$W(f) = S_s(f)\left[S_s(f) + S_v(f)\right]^{-1}, \quad (2)$$

where W is the Wiener filter, S_s and S_v are the signal and noise spectra respectively. Note that in the N-dimensional case, S_s and S_v are $N \times N$ matrices, including also cross-spectra. According to this filtering, the spectrum of the estimation error S_e can be computed as:

$$S_e(f) = S_s(f) - S_s(f)\left[S_s(f) + S_v(f)\right]^{-1} S_s(f) \quad (3)$$

and the corresponding covariance function can be derived by inverse Fourier transform. Note that equations (2) and (3) are applied seven times, i.e. once for the potential and six times for the gradients, so that the filtering of each of these data can be made independently from the filtering of the others.

2.4 Data interpolation on a spherical grid

The filtered data are transformed back to the time domain. A high degree reference model, higher than the one used for the Wiener filter, is subtracted from the data. The prediction of a spherical grid of the gravitational field functionals is then made inside equiangular blocks (of the order of 5°×5°), by least squares collocation. In this way it is possible to "homogenize" observations that are close in space but far in time, filtering out possible long period systematic effects.

The computed spherical grid is of high resolution (of the order of 0.1°×0.1°) and its radius equals the mean satellite altitude. The functional predicted in the test presented in this paper is the second radial derivative of the gravitational potential, which can be treated easily in the subsequent harmonic analysis step.

The signal covariance function is adapted to the data. From this function the signal covariance matrix C_{ss} is computed. The noise matrix C_{vv} is taken from the predicted error functions (equation 3). The prediction of a local "sub-grid" $\underline{s}_{ij}$ for the block (i, j) is:

$$\hat{\underline{s}}_{ij} = C_{s\hat{s}_{ij}}^{T} \left(C_{ss} + C_{vv}\right)^{-1} \hat{y} \,. \quad (4)$$

Note that the above formula is applied many times, once for every block, so that the whole sphere is covered. In the end the local sub-grids are assembled to form the global grid:

$$\hat{\underline{s}} = \left[\cdots \quad \hat{\underline{s}}_{ij} \quad \cdots\right]^{T} . \quad (5)$$

It has to be noted that the polar caps are not covered with observations because of the GOCE orbit inclination (i = 96.5°). The polar caps are filled by extrapolation during the gridding procedure. Actually these values are very smooth, because of the well-known property of collocation to predict smooth estimates that also tend to zero as the prediction points are more and more distant from the data points. This will be used for the harmonic analysis procedure.

2.5 Harmonic analysis on the sphere

A harmonic analysis operator is applied to the gridded data to estimate the coefficients of the spherical harmonic expansion of the gravitational potential. Two solutions are available: 1) a collocation algorithm, known as Fast Spherical Collocation (FSC) (Sansò and Tscherning, 2003) and 2) an integration method (INT) (Migliaccio and Sansò, 1989), based on the orthogonality property of the spherical harmonic functions. In the space-wise approach, both algorithms are applied and used as a mutual check method. A third solution that is based on exact Fourier analysis (Driscoll and Healy, 1994) has been investigated, that however yields results practically equivalent to integration.

The linear harmonic analysis operator H is applied on the full grid and the resulting coefficients are:

$$\hat{\underline{T}} = H\hat{\underline{s}} \,. \quad (6)$$

The absence of data on the polar caps affects the estimation of certain coefficients of the spherical harmonic expansion (Sneeuw and van Gelderen, 1997). Such a problem is usually dealt with regularization of the estimates of these coefficients. Inside the space-wise approach this regularization is achieved by filling the polar caps with smooth values, which lead to smooth estimates of the affected coefficients. Any kind of global regularization in the case of regional data gaps only is not recommended (Lemoine et al., 1998).

2.6 Iterative corrections

The synthesis of the observables (potential data and gravitational gradients) along the orbit is made with the coefficients computed at the previous step. The missing rotation terms, than concern the gradients, are computed by using these synthesized values instead of the observed gradients. The synthesized observables at iteration i are given by:

$$\tilde{\underline{y}}^{i} = S\hat{\underline{T}}^{i-1} , \quad (7)$$

where S is the linear synthesis operator. The rotation operator from GRF to LORF is applied again, this time

by setting to zero those gradients that were used the first time and by using the values $\underline{\tilde{y}}^i$ for those gradients that were set to zero the first time. In this way the initially ignored rotation terms are estimated at every iteration *i*.

The missing rotation terms is not the only reason why iterations have to be made. The second reason is that signal, especially at low frequencies where the noise of the gradients dominates, may be lost due to the Wiener filter and this can only be recovered iteratively. This is made by means of a complementary Wiener filter $W^C(f)$, defined as:

$$W^C(f) = I - W(f), \tag{8}$$

where *I* is the identity matrix. The complementary filter is applied to the Fourier transform of the synthesized values, then the computed values are transformed back to the time domain and this is the complementary correction.

Both correction terms are added to the previously filtered data and the new along track filtered data $\hat{y}^i$ at iteration *i* are computed. This results in a significant decrease of the estimation error along the orbit, at least during the first iterations. The gridding and harmonic analysis are also iterated. A new grid is computed, the harmonic analysis is repeated and from the coefficients new along track synthesized values are computed:

$$\underline{\hat{s}}_{ij}^{\ i} = C_{s\hat{s}_{ij}}^T \left(C_{ss} + C_{vv}\right)^{-1} \hat{y}^i, \tag{9}$$

$$\underline{\hat{s}}^i = \left[\cdots \quad \underline{\hat{s}}_{ij}^{\ i} \quad \cdots\right]^T, \tag{10}$$

$$\underline{\hat{T}}^i = H\underline{\hat{s}}^i, \tag{11}$$

$$\underline{\tilde{y}}^{i+1} = S\underline{\hat{T}}^i. \tag{12}$$

These values are used to compute again the rotation correction and the complementary correction, and so on. Based on numerical tests, the iterative scheme is known to converge rapidly (Migliaccio et al., 2005).

3. THE SIMULATION

3.1 The end to end data set

The latest data set provided by ESA has been used (inside the works of EGG-C) to evaluate the performance of the space-wise approach and to verify the efficiency of the software developed for this purpose. The test data set consists of observations that span a time of 60 days, at a sampling rate of 1 second. The gravity gradients in the GRF are based on the EGM96 model (Lemoine et al., 1998), up to degree and order 360, and have been contaminated with in-flight calibration noise. The satellite orbit, including positions and velocities, was simulated again using the EGM96 model up to degree and order 200. The data set contains also other information, such as orientation parameters. Among simulated data, also differential and common mode accelerations between pairs of accelerometers are provided; in particular, common mode accelerations give a direct measure of non-gravitational forces acting on the satellite and can be used in the analysis of orbit tracking data. These data represent a possible GOCE mission scenario.

3.2 Data calibration

There are three measurements for every common mode acceleration along every direction of the GRF, since there are three pairs of tri-axial accelerometers. If the measurements from different pairs of accelerometers are compared it is seen that they differ for a constant value, i.e. biases are present. If a bias is integrated in the friction estimation (equation 1) this results into a trend. Such a trend must be removed. Practically this is made by estimating the bias of the acceleration measurements.

The energy conservation algorithm is used to estimate the potential along the orbit. The estimation is compared to an a-priori model and this is sufficient to indicate if an effect similar to a trend is present. The bias model is fitted to these differences by least squares adjustment. The unknown parameters to be estimated are the energy integration constant and the accelerometer biases:

$$\underline{\xi} = \left[E_0 \quad b_x \quad b_y \quad b_z\right]^T. \tag{13}$$

The friction F is practically evaluated by the formula:

$$F(t_j) = \sum_{i=0}^{j} \underline{f}_g(t_j) \cdot \underline{v}_g(t_j) \Delta t, \tag{14}$$

where the subscript *g* denotes that the velocities and accelerations are expressed in GRF. From the last formula it is seen that the *j* row of the design matrix of the adjustment is:

$$A(j) = \left[1 \quad \sum_{i=0}^{j} v_{x_g}(t_j) \quad \sum_{i=0}^{j} v_{y_g}(t_j) \quad \sum_{i=0}^{j} v_{z_g}(t_j)\right]. \tag{15}$$

After the parameters are estimated the corrections due to the accelerometers calibration and the integration constant are added to the potential estimates.

After a low harmonic degree reference model is subtracted from the gradients it is seen, for the case of this data set, that effects of very low frequencies (like a trend, but oscillating) are present in the measurements. These effects cannot be attributed to the gravitational field (not after a reference model subtraction) and should be removed. The Wiener filter cannot be applied to this data since they do not represent a stationary time series. Therefore a calibration of the gradients is also made by approximating these effects by cubic splines and then by removing them from the data.

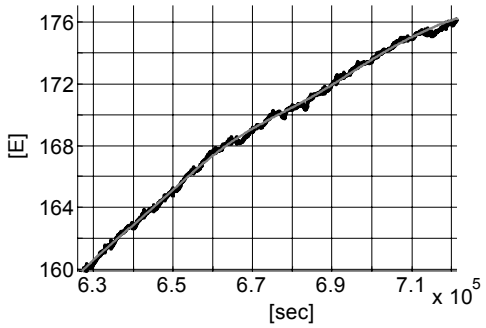

Figure 1: The gradiometric data (here the second along-track derivative T_{xx} is shown) have long wavelength noise (black) that is approximated by splines (grey).

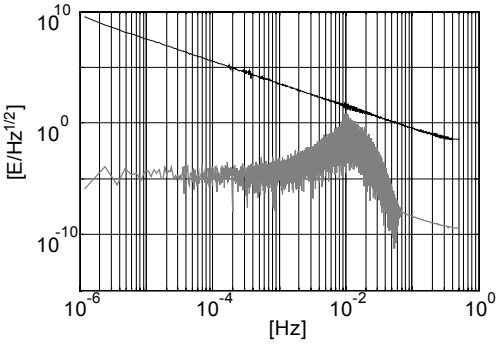

Figure 2: The spectral densities of the signal (grey) and of the observations before calibration (black) of the second along-track derivative T_{xx}.

From Figure 2 it can be seen that the data spectrum initially has a not convenient form (because the trend is known to spread along all the frequencies). In fact the "measurement bandwidth", i.e. the frequencies where the gradiometer is expected to measure with very high accuracy, is not visible, in the sense that the signal spectrum is covered by the noise spectrum. In fact a power spectrum has no sense in the case of a non stationary process. After the calibration by subtracting cubic splines this problem is overcome (see Figure 3) and the data spectrum takes the shape that was expected from the results of other experiments (Migliaccio et al., 2005).

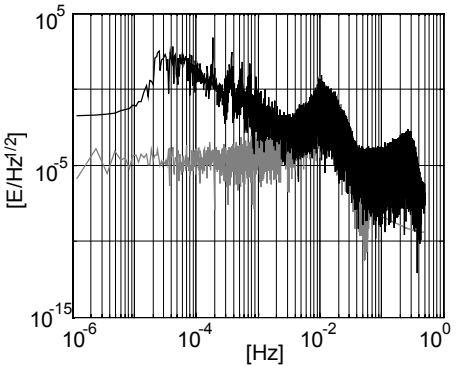

Figure 3: The spectral densities of the signal (grey) and of the observations after calibration (black) of the second along-track derivative T_{xx}.

3.3 Results of the simulation

The energy conservation method is performed along with the common mode accelerations calibration. This results in the estimation of the potential along the orbit with an accuracy of 1.6 m^2/s^2. These estimates are used for the prediction of a grid of potential values, which has an accuracy of 0.034 m^2/s^2 in the latitude interval from –83° to 83° and of 0.272 m^2/s^2 over the whole sphere. This is due to the absence of data over the polar caps.

Numerical integration is applied to this grid and spherical harmonic coefficients are recovered. These coefficients are actually corrections with respect to the EIGEN_cg03c model (Reigber et al., 2006), which was used as reference model for the computation of the grid. These estimates have very high accuracy at low degrees (Figure 4). In fact the coefficients of the first 20 harmonic degrees are not improved any more in the subsequent iterations.

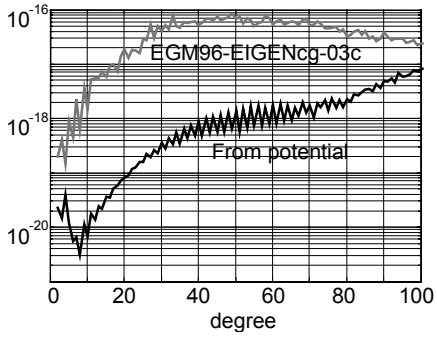

Figure 4: Error degree variances of the reference model estimated from the potential grid.

The model computed from the potential estimates is subtracted from the data along the orbit (potential and gradients) up to degree and order 50. Then the calibration of the gradients is made, as explained in paragraph 3.2. The gradients are filtered by the Wiener filter using also the information of the potential, using two dimensional Wiener filters, so that the low frequencies are better estimated. The potential is filtered using the contribution of the second radial derivatives, so that the high frequency information is improved.

The result of this filtering procedure is a very significant reduction of the error along the orbit. The error standard deviation of the gradients drops from several Eötvös (table 1) to a few milli-Eötvös (table 2). If an a-priori model is used to perform the corrections at the initial iteration, a further improvement is achieved (table 2). This probably happens because the lowest frequencies can be effectively recovered also by an a-priori model so that the convergence of the iterative procedure becomes faster. The along track potential estimates after filtering have an error standard deviation of $0.1 m^2/s^2$.

The data gridding is made by applying collocation to a moving window of 6°×6° (2° overlapping). The final grid has a resolution of 0.1°×0.1°. A global signal covariance function is used. All filtered data are under-sampled with a rate of 5 seconds (which is not critical, due to the strong time correlation of both the signal and the noise). The four most accurate gradients (table 2) are jointly treated in order to produce a spherical grid of values of T_{rr} and T_{nn} (n = north). The potential T is separately interpolated on the same spherical grid. The accuracy of these grids is quite high (table 3). The potential grid however has not really improved with respect to the first grid computed after applying the energy conservation algorithm: this means that most of the information of the potential has already been used.

Table 1: The noise standard deviation of the gradients before calibration in [E] and after calibration in [mE].

Gradient:	T_{xx}	T_{xy}	T_{xz}	T_{yy}	T_{yz}	T_{zz}
Before calibration	109	115	31	61	331	66
After calibration	156	331	101	147	450	138

Table 2: The error standard deviation in [mE] after filtering of the gradients and after correction with an a-priori model.

Gradient:	$T_{\xi\xi}$	$T_{\xi\eta}$	$T_{\xi r}$	$T_{\eta\eta}$	$T_{\eta r}$	T_{rr}
After filtering	3.5	22.0	6.0	7.8	44.1	8.7
After correction	2.7	13.6	6.3	4.8	28.3	4.9

Table 3: Error standard deviation of grids (potential in $[m^2/s^2]$ and gradients in [mE]).

grid type:	T	T_{rr}	T_{nn}
Latitude interval from -83° to 83°	0.033	1.74	1.14
Global (over the whole sphere)	0.245	12.84	8.91

Harmonic analysis is applied to the second radial derivatives grid and to the potential grid via integration. Two different estimates of the harmonic coefficients are obtained, which are afterwards combined using weights inversely proportional to the error degree variances. It is found that the contribution of the potential is small. The error degree variance of the second radial derivatives are shown in Figure 5. From these results it can be seen that the gradients carry information also on the low harmonic degree coefficients. In fact from about degree 25 on, the estimates coming from the gradients are better than those coming from the potential grid, while lower degree coefficients are held fixed to the original values estimated from the potential data.

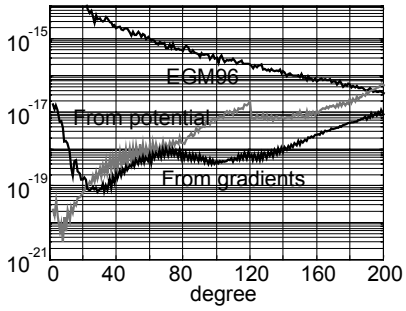

Figure 5: Error degree variances of the model computed from the potential grid (grey) and the second order degree variances grid (black).

At this point the iterations start: at each iteration the gridding and harmonic analysis procedures are repeated and the rotation correction and the complementary correction are computed and added to the data. The accuracy of the gradients after each iteration is reported in table 4. It can be seen that at iteration 3 no improvement is achieved, so the procedure is finished. The potential is not reported here, since practically it does not improve with iterations.

Table 4: error standard deviation in [mE] at every iteration of the filtering along the orbit.

Gradient:	$T_{\xi\xi}$	$T_{\xi\eta}$	$T_{\xi r}$	$T_{\eta\eta}$	$T_{\eta r}$	T_{rr}
Iteration 1	2.3	11.0	2.5	4.0	23.1	3.9
Iteration 2	2.3	11.0	2.5	3.5	23.0	3.2
Iteration 3	2.3	11.0	2.5	3.5	23.0	3.2

Table 5: error standard deviation at every iteration of the grid computation in the latitude interval from -83° to 83° (potential in [m^2/s^2] and gradients in [mE]).

Grid type:	T	T_{rr}	T_{nn}
Iteration 1	0.022	0.98	0.73
Iteration 2	0.022	0.61	0.34

Figure 6 shows that already after the first iteration there is a great improvement in the error degree variances at high degrees. However afterwards there is no further improvement and the procedure practically stops.

The empirical error (i.e. the difference of the estimated coefficients from those of EGM96) and the predicted error of the final estimated coefficients is displayed in Figures 7 and 8, showing a good agreement. The effect of the polar caps is also highlighted by the poor estimation of the low order coefficients. The commission error of the final model at degree 200 is about 2.7 cm in terms of geoid heights and 0.75 mgal in terms of gravity anomalies.

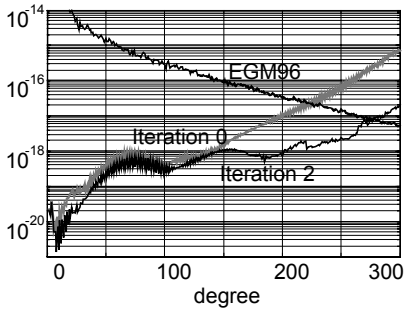

Figure 6: Error degree variances of the model computed at iteration 0 (grey) and 2 (black).

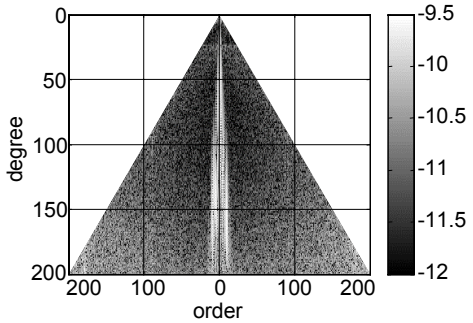

Figure 7: Empirical errors of the computed coefficients.

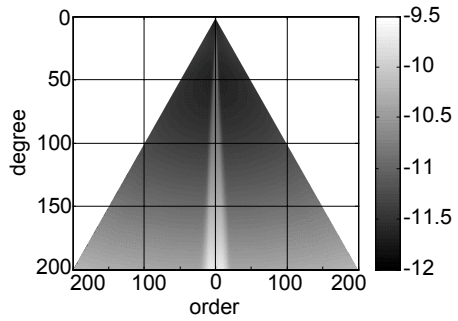

Figure 8: Predicted errors of the computed coefficients.

4. CONCLUSIONS

The solution based on the simulation presented here confirms that the space-wise approach to the GOCE data analysis is able to estimate a global model of the earth gravity field in terms of a spherical harmonics expansion up to degree 200 and beyond, with sufficient accuracy.

The simulation was valuable to assess the methodology and the software and gave the opportunity to identify ways to obtain improvements. In particular the importance of calibration methods is pointed out.

For the first time inside the space-wise approach an optimal combination of the orbit tracking data and the gradiometry data is achieved. This is obtained by using the gradients to estimate corrections for the low degree model computed from the potential data, showing that these two data sets can be combined without a-priori fixing any threshold degree.

Acknowledgement

This work was performed under ESA contract No. 18308/04/NL/NM (GOCE High-level Processing Facility).

References

1. Abrikosov, O., and P. Schwintzer (2004). Recovery of the Earth's gravity field from GOCE satellite gravity gradiometry: a case study. In: *Proc. of 2nd International GOCE User Workshop.* Frascati, Italy, March 8-10 2004.

2. Albertella, A., F. Migliaccio, M. Reguzzoni and F. Sansò (2004). Wiener filters and collocation in satellite gradiometry. In: *International Association of Geodesy Symposia, '5th Hotine-Marussi Symposium on Mathematical Geodesy'*, F. Sansò (ed), vol. 127, Springer-Verlag, Berlin, pp. 32-38.

3. Driscoll, J. R., and D. M. Healy (1994). Computing Fourier Transforms and Convolutions on the 2-Sphere. *Advances in applied mathematics*, 15, pp. 202-250.

4. ESA (1999). Gravity Field and Steady-State Ocean Circulation Mission. ESA SP-1233 (1). ESA Publication Division, c/o ESTEC, Noordwijk, The Netherlands.

5. Jekeli, C. (1999). The determination of gravitational potential differences from satellite-to-satellite tracking. *Celestial Mechanics and Dynamical Astronomy*, 75, pp. 85-101.

6. Lemoine, F.G., S.C. Kenyon, J.K. Factor, R.G. Trimmer, N.K. Pavlis, D.S. Chinn, C.M. Cox, S.M. Klosko, S.B. Luthcke, M.H. Torrence, Y.M. Wang, R.G. Williamson, E.C. Pavlis, R.H. Rapp and T.R. Olson (1998). The development of the joint NASA GSFC and NIMA geopotential model EGM96. NASA/TP-1998-206861, Goddard Space Flight Center, Greenbelt, Maryland.

7. Migliaccio, F., and F. Sansò (1989). Data processing for the Aristoteles mission. In: *Proc. of the Italian Workshop on the European Solid-Earth Mission Aristoteles.* Trevi, Italy, May 30-31 1989, pp. 91-123.

8. Migliaccio, F., M. Reguzzoni, and F. Sansò (2004a). Space-wise approach to satellite gravity field determination in the presence of coloured noise. *Journal of Geodesy*, 78, pp. 304-313.

9. Migliaccio, F., M. Reguzzoni, F. Sansò and P. Zatelli (2004b). GOCE: dealing with large attitude variations in the conceptual structure of the space-wise approach. In: *Proc. of 2nd International GOCE User Workshop.* Frascati, Italy, March 8-10 2004.

10. Migliaccio, F., M. Reguzzoni, F. Sansò and C.C. Tscherning (2004c). The performance of the space-wise approach to GOCE data analysis, when statistical homogenization is applied. *Newton's Bulletin*, 2, pp. 60-65.

11. Migliaccio, F., M. Reguzzoni, and N. Tselfes (2005). GOCE: a simulated full-gradient solution in the space-wise approach. *Proc. of the IAG2005 – Scientific Assembly*, Cairns, Australia, 22-26 August 2005. In print.

12. Pail, R., W.D. Schuh and M. Wermuth (2005). GOCE Gravity Field Processing. In: *International Association of Geodesy Symposia, 'Gravity, Geoid and Space Missions'*, C. Jekeli, L. Bastos and J. Fernandes (eds), vol. 129, Springer-Verlag, Berlin, pp. 36-41.

13. Papoulis, A. (1984). Signal analysis. McGraw Hill, New York.

14. Reigber, C., P. Schwintzer, R. Stubenvoll, R. Schmidt, F. Flechtner, U. Meyer, R. König, H. Neumayer, Ch. Förste, F. Barthelmes, S. Y. Zhu, G. Balmino, R. Biancale, J. M. Lemoine, H. Meixner and J. C. Raimondo (2006). A High Resolution Global Gravity Field Model Combining CHAMP and GRACE Satellite Mission and Surface Data: EIGEN_cg01c. *Scientific Technical Report* STR06/07.

15. Rummel, R., T. Gruber and R. Koop (2004). High Level Processing Facility for GOCE: Products and Processing Strategy. In: *Proc. of 2nd International GOCE User Workshop.* Frascati, Italy, March 8-10 2004.

16. Sansò, F., and C.C. Tscherning (2003). Fast Spherical Collocation: theory and examples. *Journal of Geodesy*, 77, pp. 101-112.

17. Sneeuw, N. and M. van Gelderen (1997). The polar gap. In: F. Sanso, R. Rummel, (eds.); *Geodetic Boundary Value Problems in View of the One Centimeter Geoid, Lecture Notes in Earth Sciences,* Springer Verlag, Berlin, pp. 559-568.

18. Tscherning, C.C. (2005). Testing frame transformation, gridding and filtering of GOCE gradiometer data by Least-Squares Collocation using simulated data. In: *International Association of Geodesy Symposia, 'A window on the Future of Geodesy'*, F. Sansò (ed), vol. 128, Springer-Verlag, Berlin, pp. 277-282.

19. Visser, P.N.A.M., N. Sneeuw and C. Gerlach (2003). Energy integral method for gravity field determination from satellite orbit coordinates. *Journal of Geodesy*, 77, pp. 207-216.